# Effect of Temperature on Hydrogen Adsorption on Pt(111), Pt(110), and Pt(100) Electrodes in 0.1 M $HClO_4$

**Roberto Gómez, José M. Orts,* Bernabé Álvarez-Ruiz, and Juan M. Feliu**

*Departament de Química Física. Universitat d'Alacant, Apartat 99, E-03080 Alacant, Spain*

*Received: April 11, 2003; In Final Form: August 25, 2003*

The dependence on temperature of the voltammetric behavior of Pt(111), Pt(100), and Pt(110) electrodes in 0.1 M $HClO_4$ has been studied. A thermodynamic analysis of the hydrogen underpotential deposition ($H_{UPD}$) has been carried out, taking into account that the adsorption process is accompanied by changes in the electrode double layer. The analysis for Pt(100) requires a previous deconvolution of the OH adsorption contribution whereas for Pt(110), the analysis is limited to high H coverages. The Pt−H bond energy values obtained for the Pt(*hkl*) electrodes agree with the values obtained in UHV. On Pt(111) and Pt(100), $\Delta G^{\circ}_{ads}(H_{UPD})$ changes linearly with coverage, with Frumkin repulsive parameters 27 and 9 kJ $mol^{-1}$, respectively. The values obtained for $\Delta S^{\circ}_{ads}(H_{UPD})$ (−48 J $mol^{-1}$ $K^{-1}$ for Pt(111), − 56 J $mol^{-1}$ $K^{-1}$ for Pt(100), and from −55 to − 70 J $mol^{-1}$ $K^{-1}$ for Pt(110)) suggest immobile hydrogen adsorption. The fact that $\Delta S^{\circ}_{ads}(H_{UPD})$ depends significantly on the crystallographic orientation suggests that the symmetry of the platinum substrate strongly influences the degree of order in the water network directly bonded to the metal surface atoms.

## 1. Introduction

Since the first papers reporting cyclic voltammograms, CV, for clean, well-ordered platinum single-crystal electrodes appeared,[1] plenty of research has been devoted to studying the behavior of the corresponding metal/solution interfaces. Significant advances have been achieved regarding their characterization at a microscopic level,[2] taking advantage of different surface science techniques such as in situ FTIRS, ECSTM, SXRS, SHG, SFG, radiotracer measurements, etc. The charge displacement method[3,4] by potentiostatic CO adsorption has also greatly helped to the disentanglement of the contributions of $H_{UPD}$ and specific anion adsorption to the total voltammetric current response for different systems. However, the understanding at the microscopic scale of the causes originating the shape of the voltammetric profiles, its dependence with various experimental parameters, and the distinction among the different processes contributing to the voltammetric current is still far from being complete. Besides the advances in new surface-sensitive techniques, the theoretical analysis of the experimental data also plays an important role. The statistical mechanical modeling of the (idealized) single-crystal electrode/electrolyte interface[5,6] has helped understand the link between the microscopic features of the system and the observed macroscopic behavior. Another, partially explored, information source is based on the analysis of the dependence of the voltammetric adsorption behavior on temperature.

Two different experimental approaches have been followed to obtain thermodynamic functions from temperature-dependent electrochemical measurements. Correspondingly, two types of electrochemical cells have been employed: isothermal and thermal cells (see, for example, ref 7). In the first case, the compartment for the reference electrode (RE) is maintained at the same temperature as the working electrode (WE) compartment. The difficulty that entails this approach is linked to the change in temperature of the reference electrode. However, if the thermodynamic analysis is based on the overall reaction, which includes the semireaction at the reference electrode, no ambiguity exists. In the case of the thermal (nonisothermal) cell, the temperature of the WE compartment changes whereas that of the RE is maintained constant. Thus the measurements are not done under equilibrium conditions (appearance of thermal-junction potentials), which requires the utilization of irreversible thermodynamics and renders difficult the obtainment of adsorption thermodynamic functions.

The isothermal cell approach was first applied to polycrystalline platinum samples by Breiter[8] and by Conway et al.[9] These authors showed how the thermodynamic functions for the adsorption of hydrogen (or of other species, such as OH) in different electrolyte media could be obtained. This provides a means for the calculation of the Pt−H bond energies and the changes in entropy linked to the hydrogen adsorption process. This latter quantity can be used, in turn, to gain information about the mobility of the adsorbate and its role in the structure of the inner region of the double layer.

The first temperature study with platinum single-crystal electrodes is due to Ross,[10,11] but unfortunately, with a degree of control of the surface order and cleanliness far from nowadays standards. In recent years, some studies about the dependence on temperature of the adsorption of hydrogen and other species on platinum single-crystal electrodes have been reported by the groups of Jerkiewicz[12−15] and Ross.[16]

In this paper, we study the temperature dependence of the voltammetric behavior for Pt(111), Pt(100), and Pt(110) electrodes in contact with a 0.1 M $HClO_4$ solution, where anion specific adsorption is considered to be absent. This situation is chosen to keep the system as simple as possible, so that information about the water (double-layer) contribution to thermodynamic quantities for $H_{UPD}$ adsorption can be drawn. Using freshly prepared electrodes and adequate cooling conditions has ensured the electrode surface order. Great attention has been paid to the cleanliness of the system, as the presence of adsorbed contaminants greatly influences the voltammetric profiles and thus the values of thermodynamic functions obtained from their analysis.[17] On Pt(111), where the potential

10.1021/jp034982g CCC: $27.50 © 2004 American Chemical Society
Published on Web 12/05/2003

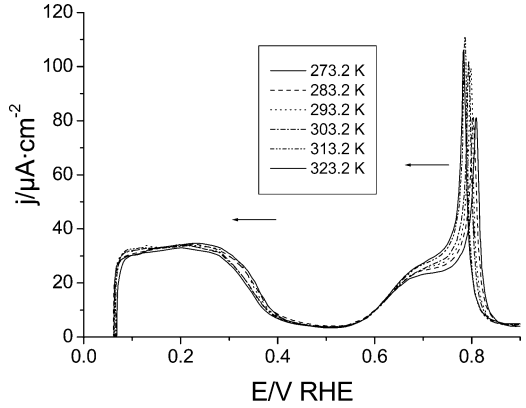


**Figure 1.** Positive scans of CV profiles for a Pt(111) electrode in a 0.1 M $HClO_4$ solution at different temperatures. Scan rate: 50 mV $s^{-1}$. Arrows indicate changes in the CV profiles associated with an increase in temperature.

regions for the adsorption of UPD hydrogen and oxygenated species do not overlap, a thermodynamic analysis will be applied to H adsorption and, in a forthcoming report, to OH adsorption. In the case of Pt(100), information on the hydrogen adsorption reaction is obtained after well-founded deconvolution of the CV contributions due to H and OH adsorbates. The deconvolution is more difficult for Pt(110), and the thermodynamic study will be restricted to the high H coverage range, where no OH adsorption is likely to take place.

## 2. Experimental Section

Platinum single-crystal surfaces were prepared as described in ref 18. A clean platinum/electrolyte interface was obtained before each voltammetric experiment, by following a standard procedure reported previously:[19] the electrode was heated in a gas + air flame and cooled in a hydrogen + argon atmosphere. Adsorption of impurities during the transfer of the sample to the controlled atmosphere of the cell was avoided by protecting the surface with a droplet of ultrapure water in equilibrium with the cooling atmosphere. Contact with the electrolyte solution was made at a controlled potential (0.10 V). Voltammetric experiments were carried out in a hanging meniscus configuration ('dipping' technique).[20]

A two-compartment, all-Pyrex electrochemical cell was used. The electrochemical cell was immersed in a water bath whose temperature was controlled to within ±0.1 K by a thermostat (Haake FK). The temperature in the water bath was measured with a platinum resistance thermometer (±0.1 K, Crison 638Pt). The experiments were carried out at different temperatures in the range $273 \leq T \leq 323$ K. Aqueous $HClO_4$ solutions were prepared from concentrated $HClO_4$ (Merck Suprapur) and ultrapure water from a Millipore system ($MiliQ_{plus}$ 185).

All potentials were measured against and are referred to a reversible hydrogen electrode, RHE, immersed in the same electrolyte, and at the same temperature that the working electrode. The counter electrode was a coiled Pt wire (99.99% purity).

The electrochemical instrumentation setup consisted of (a) an EG&G PAR Model 175 universal programmer, (b) an AMEL 551 potentiostat, and (c) a Philips PM 8133 X−Y recorder. All voltammograms were obtained at a sweep rate of 50 mV $s^{-1}$.

## 3. Results

Figure 1 shows a series of positive-going voltammetric scans obtained at a sweep rate of 50 mV $s^{-1}$ for a Pt(111) electrode in an aqueous 0.1 M $HClO_4$ solution. The negative counterparts are symmetrical with respect to the *x*-axis, as corresponds to a reversible adsorption behavior. These voltammograms were obtained at six different temperatures between 273.2 and 323.2 K, at intervals of 10 K. The profiles show features corresponding both to the adsorption/desorption of hydrogen between 0.06 and 0.40 V and to the adsorption/desorption of oxygenated species between 0.50 and 0.90 V.

**TABLE 1: Dependence on Temperature of the Charge Density Integrated between 0.06 and 0.50 V ($q^{unc}_{0.06-0.50V}/\mu C\ cm^{-2}$) and of the Charge Densities Corresponding to the Adsorption of Hydrogen ($q^{corr}_{0.06-0.50V}/\mu C\ cm^{-2}$) and Hydroxyl ($q^{corr}_{0.50-0.85V}/\mu C\ cm^{-2}$)**

| | 273 K | 283 K | 293 K | 303 K | 313 K | 323 K |
|---|---|---|---|---|---|---|
| $q^{unc}_{0.06-0.50V}/\mu C\ cm^{-2}$ | 218 | 213 | 209 | 206 | 204 | 203 |
| $q^{corr}_{0.06-0.50V}/\mu C\ cm^{-2}$ | 174 | 171 | 167 | 162 | 162 | 160 |
| $q^{corr}_{0.50-0.85V}/\mu C\ cm^{-2}$ | 108 | 110 | 110 | 109 | 113 | 111 |

Supporting electrolyte: 0.1 M $HClO_4$.

Table 1 shows raw voltammetric charge density values measured between 0.06 and 0.50 V ($q^{unc}_{0.06-0.50V}/\mu C\ cm^{-2}$) together with the values obtained after correction for the apparent double-layer (dl) contribution ($q^{corr}_{0.06-0.50V}/\mu C\ cm^{-2}$) for different temperatures. The temperature-independent current at 0.50 V was taken as the double-layer charging current chosen as baseline for carrying out the dl corrections. An alternative correction can be proposed on the basis of recent results on the Pt(111) double-layer capacity[21] and is discussed hereinafter. The charge density associated to hydrogen adsorption between 0.06 and 0.50 V increases slightly with decreasing temperatures. This is a direct consequence of the shift of the hydrogen adsorption threshold toward less positive potentials with increasing temperatures. A similar behavior has been reported in sulfuric acid solutions.[12−15]

In the potential region for hydroxyl adsorption, the peaks centered near 0.80 V (Figure 1) shift toward more positive potential values when the temperature decreases and the corresponding redox couple becomes slightly less reversible (not shown). The peak current density grows with increasing temperature, due to the narrowing of the potential region where OH adsorption takes place. Table 1 also shows the values of voltammetric charge density integrated between 0.50 and 0.85 V, corrected for the double-layer contribution ($q^{corr}_{0.50-0.85V}/\mu C\ cm^{-2}$). The hydroxyl coverage (if calculated assuming 1 electron per OH adsorbate) does not seem to depend significantly on temperature. The good constancy of the voltammetric OH adsorption charge density attests to a low level of impurities in the working solution and indicates that the changes in peak current density reflect changes in the OH adsorption behavior with temperature.

Figure 2 shows cyclic voltammetry (CV) curves obtained for a Pt(100) electrode in contact with 0.1 M $HClO_4$, at different temperatures. CV features in the region between 0.06 and 0.73 V shift toward less positive potentials when the temperature increases. The profile is also slightly sharper at the lowest temperature investigated. In that potential region, jointly with hydrogen adsorption, there is a significant charge contribution due to OH adsorption (especially at potentials above 0.4 V).[4b] The charge density values integrated between 0.06 and 0.73 V without dl correction (Table 2) are essentially independent of temperature.

Finally, Figure 3 presents CV responses for Pt(110) in 0.1 M $HClO_4$ at different temperatures. Two voltammetric peaks can be observed in the low potential range. Both peaks shift

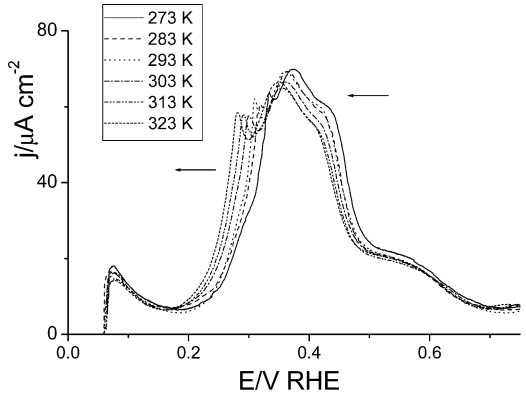


**Figure 2.** Positive scans of CV profiles for a Pt(100) electrode in a 0.1 M $HClO_4$ solution at different temperatures. Scan rate 50 mV $s^{-1}$. Arrows indicate changes in the CV profiles associated with an increase in temperature.

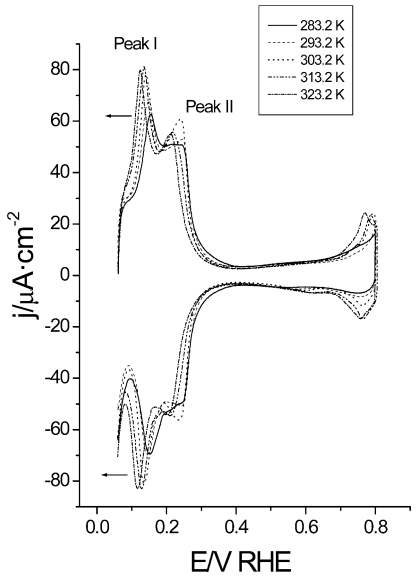


**Figure 3.** Series of CV profiles for a Pt(110) electrode in a 0.1 M $HClO_4$ solution at different temperatures. Scan rate 50 mV $s^{-1}$. Arrows indicate changes in the CV profiles associated with an increase in temperature.

**TABLE 2: Dependence with Temperature of Raw Charge Density Integrated between 0.06 and 0.75 V for Pt(100) and between 0.06 and 0.65 V for Pt(110) (Supporting Electrolyte: 0.1 M $HClO_4$)**

| | | 273 K | 283 K | 293 K | 303 K | 313 K | 323 K |
|---|---|---|---|---|---|---|---|
| Pt(100) | $q^{unc}_{0.06-0.75V}/\mu C\ cm^{-2}$ | 333 | 338 | 341 | 342 | 342 | 343 |
| Pt(110) | $q^{unc}_{0.06-0.65V}/\mu C\ cm^{-2}$ | | 215 | 218 | 223 | 231 | 235 |

toward less positive potentials when the temperature increases. An increase in temperature causes the growth of peak I whereas peak II does not vary significantly. From charge displacement results,[4] peak I can be ascribed mainly to the desorption of hydrogen whereas peak II includes contributions coming both from hydrogen desorption and from hydroxyl adsorption (positive scan). The raw voltammetric charge density (between 0.06 and 0.65 V) grows slightly as temperature increases (Table 2).

## 4. Discussion

**4.1. Thermodynamic Analysis.** We essentially follow the treatment given by Jerkiewicz and co-workers,[12−15,22] which is based on the use of a generalized adsorption isotherm. Breiter earlier reported a related procedure based on the calculation of the equivalent hydrogen pressure at each potential in the hydrogen adsorption region.[8]

The symmetry of the voltammetric profiles is indicative of a reversible adsorption behavior. Thus, the $\theta_{H_{UPD}}$ *vs E* plot (obtained from the *j* vs *E* plot) corresponds to an equilibrium situation allowing for a thermodynamic analysis.

In the potential range for hydrogen adsorption, the following reactions occur, at the working (WE) and reference electrodes (RHE), both at the same temperature:

$$\text{WE} \quad \text{Pt}(hkl) - \text{dl} + \text{H}^+(\text{aq}) + e^- \rightarrow \text{Pt}(hkl) - \text{H} - \text{dl}' \tag{1}$$

$$\text{RHE} \quad \frac{1}{2}\text{H}_2(\text{g}) \rightarrow \text{H}^+(\text{aq}) + e^- \tag{2}$$

Therefore, the global reaction studied is

$$\frac{1}{2}\text{H}_2(\text{g}) + \text{Pt}(hkl) - \text{dl} \rightarrow \text{Pt}(hkl) - \text{H} - \text{dl}' \tag{3}$$

where dl stands for the double layer characteristic of the Pt(*hkl*)/electrolyte interphase prior to the adsorption of hydrogen and dl′ stands for the double layer once hydrogen has been adsorbed.

One can obtain the following equation linking the free energy of adsorption for hydrogen, $\Delta G_{ads}(H)$, and the electrode potential (E) measured with respect to a reversible hydrogen electrode at the same temperature:[23]

$$\mu_{H_{ads}} - \frac{1}{2}\mu_{H_{2(g)}} = \Delta G_{ads}(\text{H}) = -FE \tag{4}$$

where $\mu$ stands for the chemical potential and *F* is the Faraday constant.

As the RHE operates at 1 atm pressure of hydrogen (assuming $f_{H_2} \approx 1$ atm):

$$\mu_{H_2}(T) = \mu^\circ_{H_2}(T) + RT \ln f_{H_2} \approx \mu^\circ_{H_2}(T) \equiv 0 \tag{5}$$

and therefore $\mu_{H_{ads}} = -FE\theta_{H_{UPD}}$. The value of $\theta_{H_{UPD}}(E)$, may be calculated, in the case of Pt(111), by integration of the voltammetric curve

$$\theta_{H_{UPD}}(E) = \int_{0.5}^{E} \frac{j(E') - j(0.5)}{\upsilon}\, dE' \tag{6}$$

where $\upsilon$ is the potential sweep rate. We can assume as a first approximation that the experimental current at 0.5 V can be taken as the dl correction within the H adsorption region.

As we may determine at each potential and temperature, both $\mu_{H_{ads}}$ and $\theta_{H_{UPD}}$, we may plot $\mu_{H_{ads}}$ vs $\theta_{H_{UPD}}$ for all the temperatures studied. For example, in Figure 4 (curve a) such a plot for a Pt(111) electrode at a temperature of 293 K is shown. It deviates strongly from linearity at low H coverages. Nevertheless, an almost linear function (curve b) with a nonzero slope results if we subtract from $\mu_{H_{ads}}$ the configurational term $RT \ln(\theta_H/1 - \theta_H)$ corresponding to a Langmuir isotherm.[24] This means that the chemical potential for $H_{ads}$ can be represented by

$$\mu_{H_{ads}} = \mu^\circ_{H_{ads}} + RT \ln\left(\frac{\theta_H}{1-\theta_H}\right) + r(\theta_H) \tag{7}$$

where $r(\theta_H) = \omega\theta_H$ and $\omega$ is a constant.

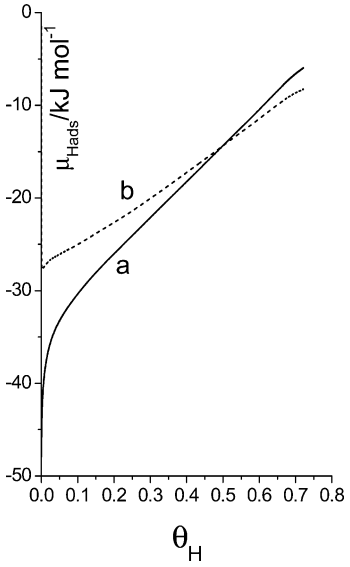


**Figure 4.** Plot of $\mu_{H_{ads}}$ vs H coverage for a Pt(111) electrode in contact with a 0.1 M $HClO_4$ solution at 293.2 K. See text for details.

Therefore the configurational term in the chemical potential seems to conform to the Langmuirian case. This is not surprising because, for H electrosorption, solvent displacement is not likely.[24b] In addition, the fact that $r(\theta_H)$, which includes all the deviations from the Langmuirian behavior, is proportional to $\theta_H$ points to the approximate validity of the Frumkin isotherm for describing H adsorption on Pt(111) electrodes in the accessible potential range.

From eqs 4, 5, and 7, it is deduced

$$\mu^\circ_{H_{ads}} - \frac{1}{2}\mu^\circ_{H_2} + r(\theta_H) = \frac{1}{2}RT \ln f_{H_2} - FE - RT \ln\left(\frac{\theta_H}{1-\theta_H}\right) \quad (8)$$

If we now define a "formal" or "apparent" standard free energy of hydrogen adsorption[24b] as

$$\Delta G^\circ_{ads}(H_{UPD}) = \mu^\circ_{H_{ads}} - \frac{1}{2}\mu^\circ_{H_2} + r(\theta_H) \quad (9)$$

Equation 8 can be written as a generalized adsorption isotherm:[25]

$$\frac{\theta_H}{1-\theta_H} = \sqrt{f_{H_2}} \exp\left(-\frac{\Delta G^\circ_{ads}(H_{UPD})}{RT}\right) \exp\left(-\frac{FE}{RT}\right) \quad (10)$$

From eq 9 it is clearly seen that the "apparent" standard free energy of adsorption depends on coverage, as it includes all the deviations from the ideal Langmuirian behavior, especially those due to lateral interactions. The generalized adsorption isotherm has been used previously in refs 12−16.

This study aims at determining the values of thermodynamic magnitudes for the underpotential deposition, UPD, of hydrogen, including $\Delta G^\circ_{ads}(H_{UPD})$, $\Delta H^\circ_{ads}(H_{UPD})$ and $\Delta S^\circ_{ads}(H_{UPD})$. The important advantage of this approach is that the only assumption done in the deduction is the separability of a Langmuirian configurational term in the adsorbate chemical potential. Any information regarding the modifications in the double layer triggered by H adsorption (mainly due to possible changes in the inner layer of chemisorbed water), will be contained in the $\Delta G^\circ_{ads}(H_{UPD})$ term in eq 10 (see eq 3).

**4.2. Pt(111) Electrodes.** As a first step in obtaining the thermodynamic properties of the hydrogen adsorption process, the dependence of hydrogen coverage on potential must be known at different temperatures. The set of coverage-potential functions is easily obtained in the case of Pt(111) by integration of the voltammetric current (eq 6), as no specific anion adsorption takes place in the potential region for the adsorption of hydrogen in 0.1 M $HClO_4$. The values of $\Delta G^\circ_{ads}(H_{UPD})$ obtained from eq 10 for different temperatures and coverages are shown in Figure 5a. An increase in $\theta_{H_{UPD}}$ causes the absolute value of $\Delta G^\circ_{ads}(H_{UPD})$ to decrease, indicating that hydrogen adsorption becomes less favored the higher its coverage.

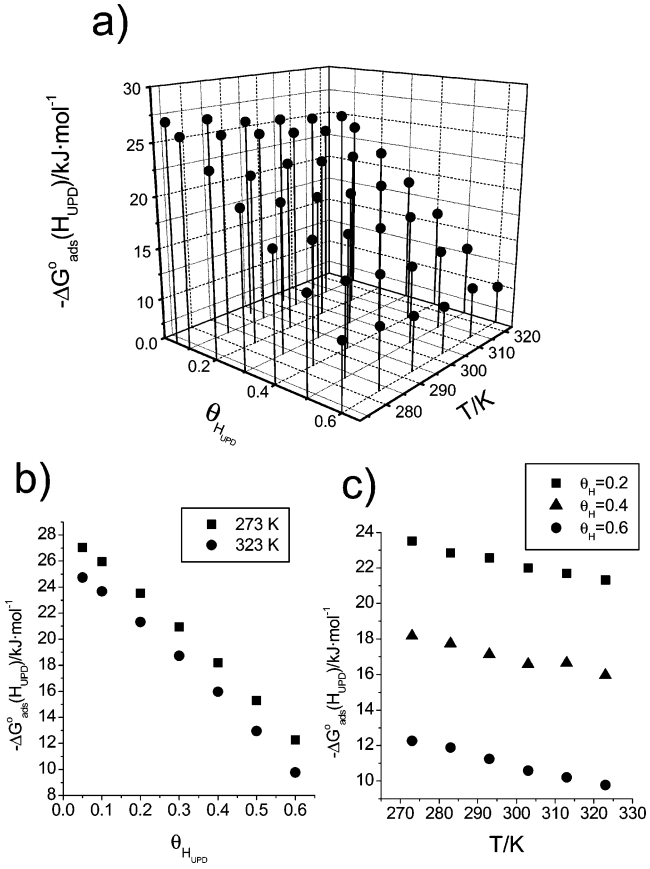


**Figure 5.** (a) Tridimensional plot of $\Delta G^\circ_{ads}(H_{UPD})$ vs temperature and hydrogen coverage ($\theta_{H_{UPD}}$), (b) dependence of $\Delta G^\circ_{ads}(H_{UPD})$ on hydrogen coverage for two different temperatures ($T_1$ = 273 K and $T_2$ = 323 K), and (c) dependence of $\Delta G^\circ_{ads}(H_{UPD})$ on temperature for three different hydrogen coverages (0.2, 0.4, and 0.6). Electrode: Pt(111). Electrolyte: 0.1 M $HClO_4$.

Figure 5b shows the dependence of $(\Delta G^\circ_{ads}(H_{UPD}))_T$ vs $\theta_{H_{UPD}}$, for two different temperatures: 273.2 and 323.2 K. The linear behavior indicates that the adsorption can be described by a Frumkin-type isotherm as anticipated.

The lateral interaction parameter $\omega$ of the Frumkin isotherm, is calculated by making the derivative of the expression for the Gibbs free energy change with respect to the hydrogen coverage at constant temperature:

$$\omega = gRT = \left(\frac{\partial \Delta G^\circ_{ads}(H_{UPD})}{\partial \theta_{H_{UPD}}}\right)_T \quad (11)$$

The values of $\omega$ calculated by using this equation do not show a significant dependence with temperature (ranging from 27.2 to 27.9 kJ $mol^{-1}$). The mean value of $\omega$ is 27.5 kJ $mol^{-1}$, corresponding to $g$ = 11.2, which indicates that there is a very strong dependence of the Gibbs energy of adsorption on hydrogen coverage. It should be kept in mind that the $\omega$ parameter includes enthalpic as well as entropic contributions.

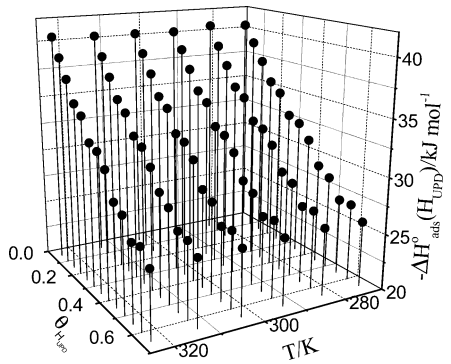


**Figure 6.** Tridimensional plot of $\Delta H^{\circ}_{ads}(H_{UPD})$ vs temperature and $\theta_{H_{UPD}}$ Electrode: Pt(111). Electrolyte: 0.1 M $HClO_4$.

Figure 5c shows the dependence of $(\Delta G^{\circ}_{ads}(H_{UPD}))_{\theta}$ on temperature for three different coverages (0.2, 0.4, and 0.6). From the slopes, an almost coverage-independent value of $-48 \pm 4$ J mol$^{-1}$ K$^{-1}$ was obtained for $\Delta S^{\circ}_{ads}(H_{UPD})$. Of course, $\Delta S_{ads}(H_{UPD})$ depends on the working electrode potential.

Once the variation of the standard adsorption entropy change is known, $\Delta H^{\circ}_{ads}(H_{UPD})$ can be calculated from

$$\Delta H^{\circ}_{ads}(H_{UPD}) = \Delta G^{\circ}_{ads}(H_{UPD}) + T\,\Delta S^{\circ}_{ads}(H_{UPD}) \quad (12)$$

Figure 6 shows $\Delta H^{\circ}_{ads}(H_{UPD})$ as a function of hydrogen coverage and temperature. The value of $|\Delta H^{\circ}_{ads}(H_{UPD})|$ for a given coverage is virtually independent of temperature. On the other hand, the $\Delta H^{\circ}_{ads}(H_{UPD})$ values are lower when $\theta_{H_{UPD}}$ is higher, ranging between $-40.6$ kJ mol$^{-1}$ for ($\theta_{H_{UPD}} = 0.05$) and $-25.8$ kJ mol$^{-1}$ (for $\theta_{H_{UPD}} = 0.65$). Therefore, the adsorption process is less exothermic for higher hydrogen coverage, as was the case for $\Delta G^{\circ}_{ads}(H_{UPD})$, which indicates again the existence of repulsive effective interactions.

An alternative method can be used for calculating $\Delta H^{\circ}_{ads}(H_{UPD})$. By taking the derivative of eq 10 with respect to $^1/_T$ at constant coverage and taking into account the Gibbs−Helmholtz equation, we obtain[25]

$$\left(\frac{d(E/T)}{d(1/T)}\right)_{\theta_{HUPD}} = \frac{-\Delta H^{\circ}_{ads}(H_{UPD})}{F} \quad (13)$$

As expected, the values of $\Delta H^{\circ}_{ads}(H_{UPD})$ obtained with this second method agree well with those reported above.

Finally, the change of standard internal energy, $\Delta U^{\circ}_{ads}(H_{UPD})$, can be calculated from

$$\Delta U^{\circ}_{ads}(H_{UPD}) = \Delta H^{\circ}_{ads}(H_{UPD}) + \frac{1}{2}RT \quad (14)$$

because $\Delta n = -^1/_2$ in our case. The values computed are similar to those found for $\Delta H^{\circ}_{ads}(H_{UPD})$ but slightly less negative (by around 1.2 kJ mol$^{-1}$).

As mentioned above, an alternative correction for the double layer could be considered on the basis of a differential capacitance value of 20 $\mu$F cm$^{-2}$ for Pt(111) in acidic solutions,[21] significantly smaller than the value used by us (68 $\mu$F cm$^{-2}$). The hydrogen coverage would be calculated according to

$$\theta^{b}_{H_{UPD}}(E) = \int_{0.5}^{E}\left(\frac{j(E')}{\nu} - C_d\right) dE' \quad (15)$$

where $C_d$ is the differential capacity for the Pt(111) electrode, taken to be 20 $\mu$F cm$^{-2}$. The coverage values determined through eq 15 are systematically higher than those calculated through eq 6, especially for high H coverages. For instance, $\theta_{H_{UPD}} = 0.60$ corresponds to a $\theta^{b}_{H_{UPD}} = 0.68$. As a result, the slopes for the curves $\Delta G^{\circ}_{ads}(H_{UPD})$ vs $\theta^{b}_{H}$ and $\Delta H^{\circ}_{ads}(H_{UPD})$ *vs* $\theta^{b}_{H}$ decrease slightly. Concretely, the value for the lateral interaction parameter, $\omega$, would change from an almost temperature independent value of 27.5 kJ mol$^{-1}$ to a mean value of 23.8 kJ mol$^{-1}$. However, no significant effect is observed for $\Delta S^{\circ}_{ads}(H_{UPD})$ values because they were shown to be independent of coverage (see above).

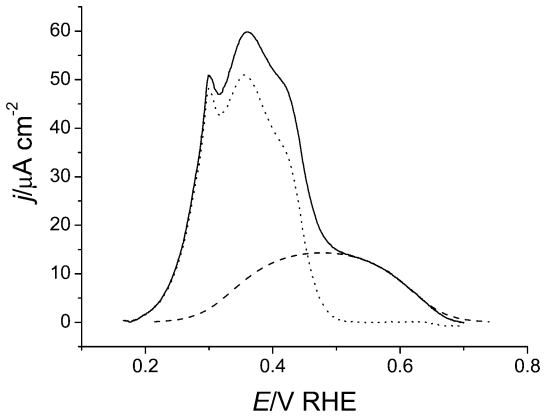


**Figure 7.** Proposed deconvolution of the double-layer corrected voltammetric profile (solid line) of Pt(100), showing two contributions: (a) hydrogen adsorption (dotted line) and (b) hydroxyl adsorption (dashed line). Electrolyte: 0.1 M $HClO_4$. Sweep rate: 50 mV s$^{-1}$. Temperature: 293.2 K.

**4.3. Pt(100) Electrode.** Although in 0.1 M $HClO_4$ the adsorption of hydrogen and hydroxyl species takes place on Pt(100) in overlapping potential ranges, the separation of both contributions is feasible if we assume that hydroxyl adsorption can be described by a Frumkin isotherm. To carry out the deconvolution analysis, the value of maximum charge density associated to the adsorption of hydroxyl species is needed. This information can be obtained from charge displacement experiments. The potential of zero total charge of Pt(100) in contact with 0.1 M $HClO_4$, at room temperature, is located at 0.43 V.[4] Integrating the CV from this latter potential up to a more positive potential where the voltammetric current (corrected for the apparent constant double-layer contribution) goes to zero, a value of 77 $\mu$C cm$^{-2}$ is obtained, which should correspond to the maximum charge density due to the adsorption of hydroxyl species.

The two contributions to the voltammetric currents due to hydrogen and hydroxyl adsorption at 293 K are shown in Figure 7. The thick solid line corresponds to the experimental voltammetric profile corrected for the double-layer contribution. The dashed line corresponds to the hydroxyl adsorption contribution and the dotted line is the contribution due to $H_{UPD}$ obtained by subtracting the OH contribution to the dl-corrected CV. The location of the hydroxyl adsorption isotherm and its shape (given by the value of the lateral interaction parameter, $\omega$) correspond to the best fit to the experimental CV in the range 0.50−0.70 V, where only hydroxyl species are believed to contribute to the voltammetric current.

Figure 8 shows the dependence of $\Delta G^{\circ}_{ads}(H_{UPD})$ on temperature and $\theta_{H_{UPD}}$. The mean value of $\Delta S^{\circ}_{ads}(H_{UPD})$ obtained for Pt(100) is $-56 \pm 4$ J mol$^{-1}$ K$^{-1}$, independently of coverage as deduced from the linearity of curve $\Delta G^{\circ}_{ads}(H_{UPD})$ vs $T$ (Figure 8b). From Figure 8c the lateral effective interaction parameter for hydrogen adsorption on Pt(100), is 9 kJ mol$^{-1}$ ($g = 4$), still repulsive but much smaller than in the case of Pt(111).

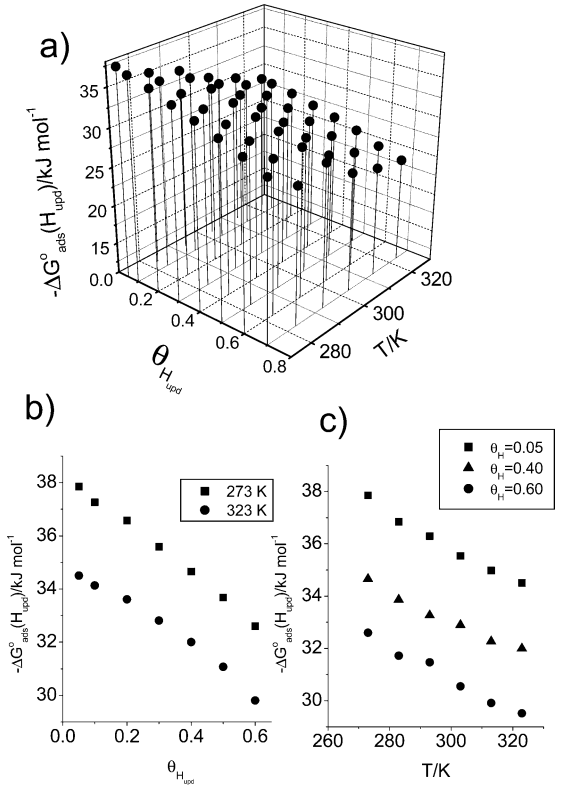


**Figure 8.** (a) Tridimensional plot of $\Delta G^{\circ}_{ads}(H_{UPD})$ vs temperature and hydrogen coverage ($\theta_{H_{UPD}}$), (b) dependence of $\Delta G^{\circ}_{ads}(H_{UPD})$ with hydrogen coverage for two different temperatures ($T_1 = 273$ K and $T_2 = 323$ K), and (c) dependence of $\Delta G^{\circ}_{ads}(H_{UPD})$ on temperature for three different hydrogen coverages (0.05, 0.40, and 0.60). Electrode: Pt(100). Electrolyte: 0.1 M $HClO_4$.

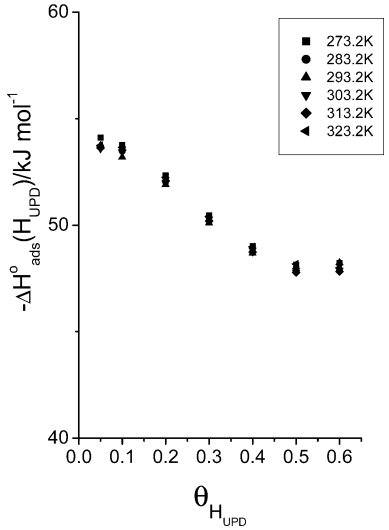


**Figure 9.** Dependence of $\Delta H^{\circ}_{ads}(H_{UPD})$ with hydrogen coverage for several temperatures. Electrode: Pt(100). Electrolyte: 0.1 M $HClO_4$.

The $\Delta H^{\circ}_{ads}(H_{UPD})$ values range from $-53$ kJ mol$^{-1}$ (for $\theta_{H_{UPD}} = 0.05$) to $-48$ kJ mol$^{-1}$ (for $\theta_{H_{UPD}} = 0.60$), as seen in Figure 9. Hydrogen adsorption is more favorable at lower coverage and the variation of $\Delta H^{\circ}_{ads}(H_{UPD})$ with coverage for Pt(100) is not as important as in the case of Pt(111). Recent results[26] give alternative values for the Pt(100) differential capacity in perchlorate solutions but only in the pH range from 4 to 7. Accepting similar corrections for 0.1 M $HClO_4$ would lead to results akin to those shown in Figure 9, although with a smaller slope.

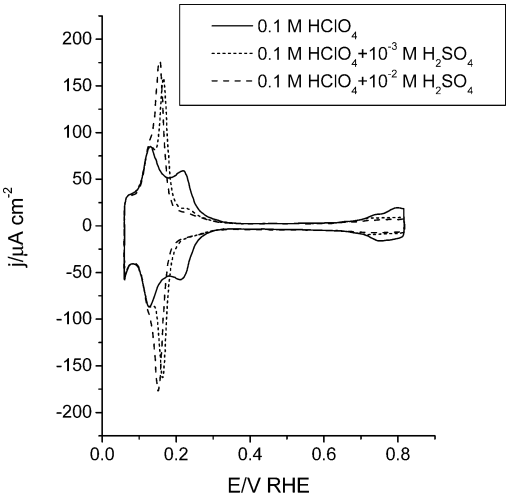


**Figure 10.** Voltammetric profiles for a Pt(110) electrode in a 0.1 M $HClO_4$ solution and with the addition of $10^{-3}$ or $10^{-2}$ M $H_2SO_4$. Scan rate: 50 mV s$^{-1}$. Room temperature.

**4.4. Pt(110) Electrode.** The separation of the contributions of hydrogen and hydroxyl adsorption to the voltammetric current is not obvious in the case of Pt(110), which impedes a reliable estimation of the thermodynamic adsorption quantities over wide coverage ranges. However, for high hydrogen coverages $\Delta G^{\circ}_{ads}(H_{UPD})$ and $\Delta H^{\circ}_{ads}(H_{UPD})$ can be obtained from eqs 10 and 12. Finally, $\Delta S^{\circ}_{ads}(H_{UPD})$ values can be also obtained by isolating $\Delta G^{\circ}_{ads}(H_{UPD})$ in eq 10 and making its partial derivative with respect to temperature at constant hydrogen coverage:

$$\Delta S^{\circ}_{ads} = -\left(\frac{\partial \Delta G^{\circ}_{ads}}{\partial T}\right)_{\theta_H} = F\left(\frac{\partial E}{\partial T}\right)_{\theta_H} + R \ln\left(\frac{\theta_H}{1-\theta_H}\right) \quad (16)$$

The value obtained at room temperature for the potential of total zero charge of Pt(110) in 0.1 M $HClO_4$ by means of charge displacement experiments and subsequent integration of the CV is 0.23 V.[4] Therefore, peak I in Figure 3 can be attributed exclusively to hydrogen adsorption. In fact, Figure 10 shows the voltammetric profiles for Pt(110) in the absence and in the presence of (bi)sulfate anion in the working solution ($10^{-3}$ or $10^{-2}$ M $H_2SO_4$). The coincidence of the curves in the low potential range up to the first peak indicates the absence of specific adsorption of anions in that potential range, supporting the notion that in this region the dl-corrected current is due exclusively to $H_{UPD}$ adsorption.

The CV is integrated in the negative going scan from the minimum just positive to the onset of hydrogen evolution, up to the potential of peak I. Admittedly, we assume for this orientation that the H coverage at the hydrogen evolution reaction threshold (current minimum around 0.09 V) is equal to unity for all temperatures, which agrees with charge displacement measurements.[4] After correction for the double-layer contribution, the H coverage is calculated at the peak I potential (around 0.14 V) to be $0.65 \pm 0.03$ for all temperatures.

Values for $\Delta G^{\circ}_{ads}(H_{UPD})$ at $\theta_{H_{UPD}} = 0.65$ range from $-16.1$ kJ mol$^{-1}$ at 283.2 K to $-13.3$ kJ mol$^{-1}$ at 323.2 K. As for $\Delta H^{\circ}_{ads}(H_{UPD})$ a temperature-independent value of $-36.1$ kJ mol$^{-1}$ was obtained ($\theta_{H_{UPD}} = 0.65$). The estimation of $(\partial E/\partial T)_{\theta_{H}=0.65}$ is done as $(\partial E_p/\partial T)_{\theta_{H(E_p)}} = 0.79$ mV K$^{-1}$, where $E_p$ is the peak I potential. The value obtained for $\Delta S^{\circ}_{ads}(H_{UPD})$ is $-70 \pm 5$ J mol$^{-1}$ K$^{-1}$ ($\theta_{H_{UPD}} = 0.65$).

We have extended these calculations to coverages higher than 0.65 assuming that $\theta_{UPD} = 1$ at the minimum in the negative-going scan. Results for $\Delta G^{\circ}_{ads}(H_{UPD})$ are presented in Figure 11

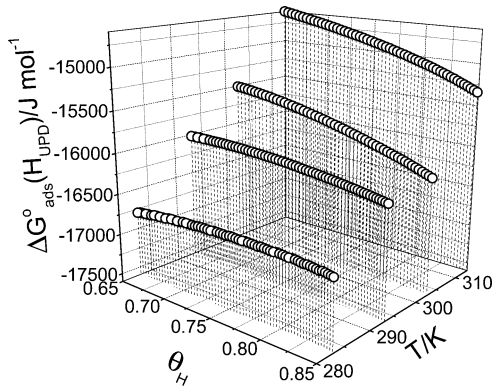


**Figure 11.** Dependence of $\Delta G^{\circ}_{ads}(H_{UPD})$ on temperature and hydrogen coverage ($\theta_{H_{UPD}}$) for a Pt(110) electrode in contact with 0.1 M $HClO_4$.

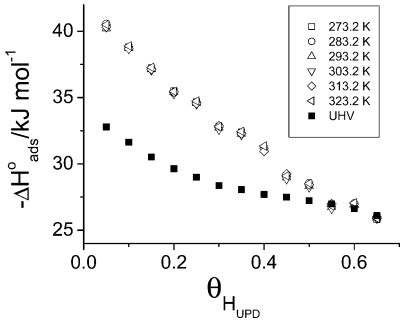


**Figure 12.** Comparison of $\Delta H^{\circ}_{ads}(H_{UPD})$ (obtained under electrochemical conditions) with $\Delta H^{\circ}_{ads}(H)$ (under UHV conditions) taken from ref 32.

and refer to a very narrow range of coverages as for $\theta_{H_{UPD}} >$ 0.80 interference from the hydrogen evolution reaction begins to be noticeable. In any case, $\Delta S^{\circ}_{ads}(H_{UPD})$ tends to be less negative as $\theta_{H_{UPD}}$ increases: for a coverage as high as 0.8, the value of entropy change is $-55$ J mol$^{-1}$ K$^{-1}$. On the other hand, it is remarkable that weak attractive lateral interactions are observed in contrast with the behavior of Pt(100) and Pt(111). A maximum lateral attractive interaction of $-4$ kJ mol$^{-1}$ is found at 323 K.

**4.5. Comparison with Results for H Adsorption at the Pt(*hkl*)/Gas Interphase.** To gain information about the effect of the presence of an electrical double layer on the hydrogen adsorption process (and viceversa), we compare values for the thermodynamic functions of H adsorption in both environments.

Figure 12 shows the comparison of our results for $\Delta H^{\circ}_{ads}(H_{UPD})$ with UHV data for the Pt(111) surface. Differences observed at low coverages amount to 7 kJ mol$^{-1}$ (the adsorption being less exothermic in UHV), but identical values are obtained in UHV and under electrochemical conditions at high hydrogen coverages. The comparison can be made through the following cycle:

$$\begin{array}{ccc} Pt(hkl) & \xrightarrow{+solution} & Pt(hkl)-dl \\ +1/2\ H_2 \downarrow & & +1/2\ H_2 \downarrow \\ Pt(hkl)-H & \xrightarrow{+solution} & Pt(hkl)-H-dl' \end{array} \qquad (17)$$

from which we deduce

$$\Delta H^{\circ}_{ads}(H_{UPD}) = \Delta H^{\circ}_{ads}(H) + \Delta H^{\circ}_{f}(dl') - \Delta H^{\circ}_{f}(dl) \quad (18)$$

$$\delta(\Delta H^{\circ}_{ads}) = \Delta H^{\circ}_{ads}(H_{UPD}) - \Delta H^{\circ}_{ads}(H) = \delta(\Delta H^{\circ}_{f}(dl)) = \Delta H^{\circ}_{f}(dl') - \Delta H^{\circ}_{f}(dl) \quad (19)$$

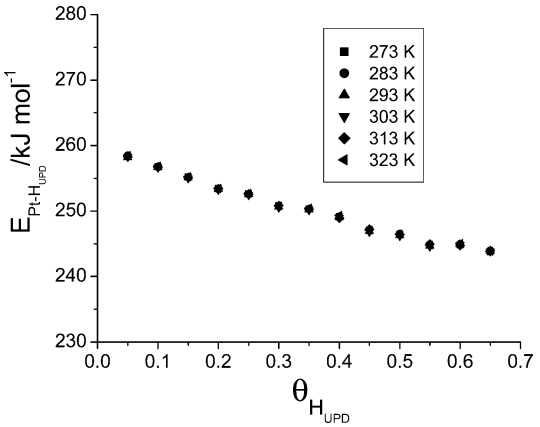


**Figure 13.** Dependence of $E_{Pt-H_{UPD}}$ on hydrogen coverage for different temperatures. Electrode: Pt(111). Electrolyte: 0.1 M $HClO_4$.

Interestingly, from the similarity of the $\Delta H^{\circ}_{ads}$ values for Pt(111) in both environments, we can conclude that $\delta(\Delta H^{\circ}_{ads})$, the change in enthalpy associated with the formation of the double layer, is not affected to an important extent by the chemisorption of hydrogen at constant potential on the Pt(111) electrode surfaces. However, it can be seen from Figure 12 that $\Delta H^{\circ}_{f}(dl) > \Delta H^{\circ}_{f}(dl')$ by a few kJ mol$^{-1}$ for low H coverages. As we are dealing with H chemisorption, the changes in the enthalpy of dl formation can be considered to come mostly from modifications in the inner layer. No influence of perchlorate anions is expected, as they are not present in the inner double layer (absence of specific adsorption). In a first approach we can relate $\Delta H^{\circ}_{f}(dl)$ to the average change in the number of hydrogen and adsorption bonds experienced by each water molecule in the double layer (especially in the inner layer), taking as a reference the situation in the bulk. We can conclude that the average number of hydrogen bonds or Pt$-H_2O$ bonds (of similar energy[27]) associated with each water molecule in the layer adjacent to the Pt(111) electrode does not vary much upon hydrogen adsorption. For low H coverages, however, the number of hydrogen/adsorption bonds of water increases slightly upon H adsorption, which could reflect an increase of the number of water molecules in the inner layer or the formation of solvated hydronium ions from H adatoms.[28−30] These tentative considerations could be more precisely stated by means of quantum chemical and statistical mechanical studies of the interphasial system.

The energy of the Pt$-H_{UPD}$ bond can be calculated by using a thermodynamic cycle including the reactions occurring at the working and reference electrodes (reactions 1 and 2)[22] that leads to the expression

$$E_{Pt-H_{UPD}} \cong \frac{1}{2}D_{H_2} - \Delta U^{\circ}_{ads}(H_{UPD}) \approx \frac{1}{2}D_{H_2} - \Delta H^{\circ}_{ads}(H_{UPD}) \qquad (20)$$

In this calculation the double-layer contribution to the enthalpy is implicitly neglected, which stresses its qualitative nature. A value of +436 kJ mol$^{-1}$ is taken[31] for the dissociation energy of the $H_2$ molecule. Figure 13 shows the $E_{Pt-H_{UPD}}$ versus $\theta_{H_{UPD}}$ plots at a series of temperatures. As can be seen, $E_{Pt-H_{UPD}}$ is independent of temperature but shows a slight dependence with hydrogen coverage: it decreases from 258 kJ mol$^{-1}$ (for $\theta_{H_{UPD}} = 0.05$) to 243 kJ mol$^{-1}$ (for $\theta^{b}_{H_{UPD}} = 0.73$ if the coverage is calculated with eq 15). These values agree with those obtained in UHV, which range between 237 and 255 kJ mol$^{-1}$.[32] Different groups have used DFT for calculating the Pt(111)$-$H energy. Podkolzin et al.[33] obtained values around 262 ± 1 kJ mol$^{-1}$ for

different kinds of adsorption sites. Watson et al.[34] obtained values between 260.5 kJ mol$^{-1}$ (bridge site) and 264 kJ mol$^{-1}$ (fcc hollow site). The values obtained for $E_{Pt-H_{UPD}}$ are similar despite the very different experimental conditions, electrochemical and ultrahigh vacuum. This does not mean, however, that double-layer effects are totally negligible because, as discussed later, changes of the solvent structure in the inner region of the double layer may occur. In fact, the small difference in $\Delta H^\circ_{ads}(H_{UPD})$ in both environments and ascribed to dl contributions is obviously reproduced in $E_{Pt-H_{UPD}}$ calculations.

With regard to the Pt(100)−H bond (Figure 14), its energy, $E_{Pt-H_{UPD}}$, is found to be independent of temperature, as expected, and slightly dependent on coverage: it decreases by less than 3% from 272 ($\theta_{H_{UPD}} = 0.05$) to 266 kJ mol$^{-1}$ ($\theta_{H_{UPD}} = 0.60$). Comparison with the UHV values of $\Delta H^\circ_{ads}(H)$ and the Pt(100)−H bond energy (263.5 kJ mol$^{-1}$),[35] reveals very small differences despite the disparity in experimental conditions. This result supports the enthalpic contribution due to the modification of the solvent structure at the inner region of the double layer also being negligible in the estimation of Pt(100)−H bond energy.

Finally, the values for the case of Pt(110) in the UHV environment range from 253 to 270 kJ mol$^{-1}$.[35] On the basis of the value reported above for $\Delta H^\circ_{ads}(H_{UPD})$, a value of 254 kJ·mol$^{-1}$ is deduced for $E_{Pt-H_{UPD}}$, for a relatively high H coverage (around 0.65), which is fully compatible with values for the Pt(110)/gas interface.

Although of limited importance for enthalpic considerations, the existence of a double layer and the change in its structure upon hydrogen adsorption need to be addressed to discuss the values of standard entropy changes for H adsorption. It is generally accepted that water in the inner part of the double layer has a higher degree of order (lower level of mobility) than water in the bulk of the working solution. The similarity of the Pt−Pt distance (0.278 nm) with that of O atoms in ice structures[36] and the strength of hydrogen bonds (around 8−9 times $kT$ at room temperature) strongly favor the formation of ordered domains of a H-bonded network of adsorbed water molecules over the Pt electrodes. This is particularly true at Pt(111) where the symmetry and interatomic distances within the outmost atomic plane of the substrate are optimal for the formation of a 2D "ordered" water network, because of the geometry of the water molecule.

An analysis of the entropy values for $H_{UPD}$ adsorption can be attempted by using the cycle (17) presented above. The following expression for $\Delta S^\circ_{ads}(H_{UPD})$ is deduced:

$$\Delta S^\circ_{ads}(H_{UPD}) = \Delta S^\circ_{ads}(H) + S^\circ_{dl'} - S^\circ_{dl} \qquad (21)$$

where $S^\circ_{dl'}$ and $S^\circ_{dl}$ refer to the absolute standard entropy values of the double layer with and without adsorbed hydrogen, respectively.

Taking into account that hydrogen adsorbs dissociatively, a statistical mechanical calculation[37,38] can be made for the expected value of $\Delta S^\circ_{ads}(H_{UPD})$ corresponding to an ideal adlayer in the limiting cases of a fully mobile hydrogen adlayer or a totally immobile one. In the first case the (differential) entropy for the adsorbed layer, which includes configurational and translational contributions[37a] is given by

$$S^\circ(H) = R\left[1 + \ln\left(\frac{2\pi m_H kT}{h^2}\frac{1}{c_s\theta^\circ_H}\right)\right] \qquad (22)$$

where $m_H$ is the atomic mass for H, $k$ and $h$ are Boltzmann and

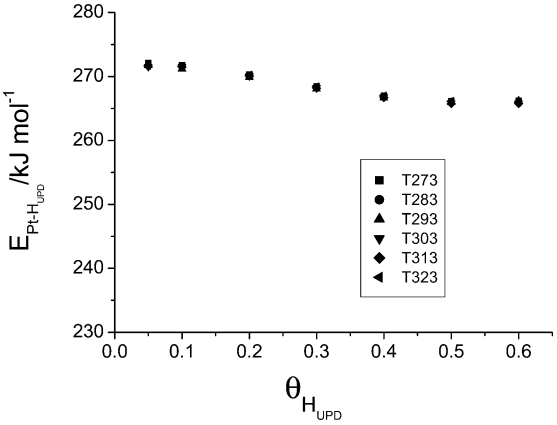


**Figure 14.** Dependence of $E_{Pt-H_{UPD}}$ on hydrogen coverage for different temperatures. Electrode: Pt(100). Electrolyte: 0.1 M $HClO_4$.

Planck constants, $c_s$ corresponds to the surface density of adsorption sites and $\theta^\circ_H = {}^1/_2$ according to our choice for the standard state. For a totally immobile adlayer we will have both configurational and vibrational contributions. The configurational entropy is given by

$$S^\circ_{config}(H) = -R\ln\left(\frac{\theta^\circ_H}{1-\theta^\circ_H}\right) \qquad (23)$$

resulting in a zero contribution for our choice of standard state for the adsorbate $\theta^\circ_H = {}^1/_2$, and the vibrational contribution is given by

$$S^\circ_{vib}(H) = R\sum\left[\frac{h\nu_i}{kT}\frac{1}{\exp(h\nu_i/kT)-1} - \ln[1-\exp(h\nu_i/kT)]\right] \qquad (24)$$

where the summation extends over the vibrational modes (of frequencies $\nu_i$) of the Pt−H bond (both parallel and perpendicular to the surface). Values for these frequencies can be found in the literature as far as we know for Pt(111)[39] and Pt(110).[40]

It should be mentioned that in these calculations no particular type of adsorption site for hydrogen is assumed and that the surface is supposed to be homogeneous (all adsorption sites, of the same type, are equivalent). Once these adlayer entropies are computed the calculation of the theoretical $\Delta S^\circ_{ads}(H)$ can be done as

$$\Delta S^\circ_{ads}(H) = S^\circ_{ads}(H) - \frac{1}{2}S^\circ(H_{2,g}) \qquad (25)$$

The standard entropy of gaseous hydrogen ($S^\circ(H_{2,g})$) is tabulated.[31] The calculated values for the adlayer and adsorption entropies as well as the experimental values for $\Delta S^\circ_{ads}(H_{UPD})$ are given in Table 3.

The experimental $\Delta S^\circ_{ads}(H_{UPD})$ values are $-56 \pm 4$ J mol$^{-1}$ K$^{-1}$ for Pt(100), $-45 \pm 4$ J mol$^{-1}$ K$^{-1}$ for Pt(111), and from $-55$ to $-70 \pm 5$ J mol$^{-1}$ K$^{-1}$ for the Pt(110) surface, depending on coverage. It is noteworthy that in this case the value of dl capacity assumed for calculating hydrogen coverages is not significant, as $\Delta S^\circ_{ads}(H_{UPD})$ does not vary with coverage in the cases of Pt(111) and Pt(100). The first two values are intermediate between the immobile and mobile reference values, whereas some of the values for Pt(110) are even more negative than the value for the immobile adlayer. It is clearly seen from the table that the reference theoretical values are almost insensitive to the particular substrate surface structure. Conversely, there exist significant differences between the experimental values for the

**TABLE 3: Calculated Values for Entropy of the H Adlayer and Experimental Values for the Change of Entropy for the Hydrogen Adsorption Process on Pt(111), Pt(100), and Pt(110)**

| | Pt(111) | Pt(100) | Pt(110) |
|---|---|---|---|
| $S°(H)_{mobile}$/J mol$^{-1}$ K$^{-1}$ | 29.7 | 30.9 | 33.8 |
| $S°(H)_{immobile}$/J mol$^{-1}$ K$^{-1}$ | 4.7[a] | | 4.0[b] |
| $\Delta S°_{ads}(H)_{mobile}$/J mol$^{-1}$ K$^{-1}$ | −35.7 | −34.5 | −31.6 |
| $\Delta S°_{ads}(H)_{mobile}$/J mol$^{-1}$ K$^{-1}$ | −60.7 | −61[c] | −61.5 |
| $\Delta S°_{ads}(H_{UPD})$/J mol$^{-1}$ K$^{-1}$ | −48 | −56 | −70 |

[a] Data taken from ref 39. [b] Data taken from ref 40. [c] Entropy for the immobile adsorbed layer is taken to be 4.4 J mol$^{-1}$ K$^{-1}$.

three platinum surface orientations, which should be attributed mainly to the changes in the structure of the inner region of the double layer upon hydrogen adsorption, i.e., to the existence of a term ($S°_{dl'} - S°_{dl}$). The fact that hydrogen adsorption can be considered as immobile agrees with hydrogen adsorbed on a rather deep potential well (interstitial sites). Hydrogen adatoms need to acquire a high amount of energy to surmount the potential energy barrier for diffusion at the surface, especially when a strongly adsorbed network of hydrogen-bonded water molecules exists, blocking the on-top adsorption positions.

The adsorption of hydrogen can exert a significant effect on the structure of the inner layer, leading probably to some degree of disorder/mobility in the adsorbed water network. If this is the case, the term ($S°_{dl'} - S°_{dl}$) is expected to have a positive value. In the framework of this discussion it is informative to estimate an expected value for the double-layer entropic term. Let us consider the extreme case where, prior to hydrogen adsorption (dl), the water in the inner layer presents a rigid ice-like structure, whereas after hydrogen adsorption (dl′) the configuration (mobility) is that of liquid water at 0 °C. The entropy for such a process can be estimated form the enthalpy of melting for the ice−water phase transition. For the bulk 3D phase transition case an entropy increase of +22 J mol$^{-1}$ K$^{-1}$ occurs upon melting (corresponding to a molar heat of melting of 6.02 kJ mol$^{-1}$ [31]), as calculated from $\Delta S_{fus} = \Delta H_{fus}/T_{fus}$. In the case of the double layer, the expected increase of entropy would be lower, as restrictions to translational and librational movement due to the presence of the solid electrode surface persist. In that case, and taking into account the different dimensionality of the system undergoing disordering, the entropy change for the 2D chemisorbed water adlayer can be roughly estimated to amount to a value around two-thirds of that for the 3D case (around 15 J mol$^{-1}$ K$^{-1}$). This value is close to the difference between the entropy change corresponding to $H_{UPD}$ and to the ideal immobile H adsorption in a vacuum, for the case of Pt(111).

Cryogenic UHV experiments also provide additional support to the existence of some disordering of the dl structure triggered by the adsorption of H. Upon hydrogen adsorption, the HREELS signals characteristic of an ordered water structure, become wider and less intense.[28−30] In addition, their frequencies shift toward lower wavenumbers. This type of behavior indicates a modification of the water adlayer structure toward a more disordered state when hydrogen adsorbs.

Therefore, $\Delta S°_{ads}(H_{UPD})$ is lower in the case of Pt(111) because an ordered structure of water initially exists, whose order is disrupted, seemingly to a significant extent by the adsorption of hydrogen. The value of $\Delta S°_{ads}(H_{UPD})$ for Pt(100) is more negative than that of Pt(111). This is probably linked to the structure of the water adlayer, which on Pt(100) is supposed to be not as ordered as in the case of Pt(111), due to the 4-fold symmetry of the Pt(100) surface atomic arrangement, less favorable for the formation of an extended hydrogen bonded network of adsorbed water. In this case the adsorption of hydrogen is expected to modify less significantly the degree of structural order of a relatively disordered inner layer, thus $(S°_{dl'} - S°_{dl})_{Pt(100)} < (S°_{dl'} - S°_{dl})_{Pt(111)}$ and the value of $\Delta S°_{ads}(H_{UPD})$ is closer to $\Delta S°_{ads}(H)$ for an immobile adlayer.

**TABLE 4: Comparison of the Values for the Change in Thermodynamic Functions for the Process of Hydrogen Adsorption on Pt(111) in 0.1 M $HClO_4$[a]**

| | present study | data of ref 16 |
|---|---|---|
| $\Delta G°_{ads}(H_{UPD})$/kJ mol$^{-1}$ | −27 ↔ −8 | −28 ↔ −10 |
| $\Delta S°_{ads}(H_{UPD})$/J mol$^{-1}$ K$^{-1}$ | −54 ↔ −41 | −49 ↔ −45 |
| $\Delta H°_{ads}(H_{UPD})$/kJ mol$^{-1}$ | −41 ↔ −26 | −41 ↔ −24 |
| $E_{Pt-H_{UPD}}$/kJ mol$^{-1}$ | 243 ↔ 258 | 240 ↔ 250 |
| $\omega$/kJ mol$^{-1}$ | 27 ↔ 28 | 4 ↔ 36 |

[a] In the first column the coverage studied ranges from 0.05 to 0.60, for temperatures between 273 and 323 K, whereas in the second column coverage ranges from 0.05 to 0.50, and temperatures between 273 and 333 K.

For Pt(110), $\Delta S°_{ads}(H_{UPD})$ is equal to −70 J mol$^{-1}$ K$^{-1}$ ($\theta_{H_{UPD}} = 0.65$) although it decreases for higher coverages. This value is even more negative than that calculated for the immobile hydrogen adsorption case. The strong difference with Pt(111) and Pt(100) can be rationalized as a logical consequence of a significantly more disordered water adlayer in the absence of adsorbed hydrogen, with minimal changes in its degree of disorder upon hydrogen adsorption. This behavior is probably linked to the corrugated, strongly anisotropic surface structure of Pt(110), where a bidimensional hydrogen-bonded water network seems to be strongly disfavored.

Finally, we compare the data presented above with results found in the bibliography. The adsorption of hydrogen on Pt(111) electrodes in contact with the same working solution has been studied in a recent paper.[16] In Table 4 we compare our data with that of ref 16 for 0.1 M $HClO_4$. No significant differences are observed, except for the bigger variation of the value of the lateral interaction Frumkin parameter in ref 16.

**4.6. Effects of Anion Adsorption on Hydrogen Adsorption.** In their pioneering work, Breiter and co-workers[8,41] pointed out that on polycrystalline platinum the anions present in the working solution exert an important effect on the adsorption heat of hydrogen, especially for low coverages. In light of recent investigations[4] the direct contribution of specifically adsorbed anions to the voltammetric charge in the so-called hydrogen region has been evidenced. This fact casts serious doubts on the actual significance of the values determined by Breiter et al. at low coverages.

In the case of Pt(111) electrodes, there is a clear separation between the regions of hydrogen and anion adsorption, which allows us to investigate the genuine effect that anions may play in the adsorption of hydrogen. Given that the voltammetric profile for H adsorption ($E < 0.32$ V RHE) is virtually identical in sulfuric and perchloric acid solutions,[42] we may infer that no significant effect on the Frumkin lateral interaction parameter of hydrogen is caused by the presence of (bi)sulfate in the working solution.

Temperature-dependent data have been obtained for Pt(111) electrodes in contact with a 0.5 M $H_2SO_4$ solution by Zolfaghari and Jerkiewicz.[43] The values obtained for $\Delta S°_{ads}(H_{UPD})$ and $\omega$ are similar to those presented here. However, some differences exist. Our results indicate that $\Delta S°_{ads}(H_{UPD})$ and $\omega$ are not significantly dependent on the temperature, in contrast with the data presented by the aforementioned authors. Moreover, the value of $\Delta S°_{ads}(H_{UPD})$ on Pt(111) obtained by us is −48 J mol$^{-1}$

$K^{-1}$, significantly lower than those presented by Zolfaghari et al., which range between −80 and −62 J $mol^{-1}$ $K^{-1}$. In a more recent report, Markovic et al.[16] analyzed the effect of anions and pH on the thermodynamics of hydrogen adsorption on low-index single-crystal platinum electrodes in acidic media. They concluded that neither the anion nor the pH affected in a significant way the thermodynamic state functions for H adsorption. Thus, there seems to be no effect of the anions (perchlorate or bisulfate) on the adsorption of hydrogen on Pt(111), as in this case a clear separation exists between the potential ranges for adsorption of hydrogen and anions.

In the case of Pt(100) and Pt(110) (especially in the low hydrogen coverage range) electrodes, the effect of anions (i.e., (bi)sulfate) is difficult to assess because the potential regions for both adsorption processes are overlapped, which precludes any quantitative analysis, as there is no sound basis to perform a deconvolution of both contributions.

## 5. Conclusions

We have studied from a thermodynamic point of view the effect of temperature on the hydrogen adsorption process:

$$\frac{1}{2}H_2 + Pt(hkl) - dl \rightleftarrows Pt(hkl) - dl'$$

at platinum electrodes with basal orientations. The approach, based on a generalized electrochemical adsorption isotherm, allows the calculation of $\Delta G^\circ_{ads} = \Delta G^\circ_{ads}(\theta,T)$ without introducing additional assumptions. From an analysis of this function other thermodynamic quantities ($\Delta H^\circ_{ads}$, $\Delta U^\circ_{ads}$ and $\Delta S^\circ_{ads}$) can be estimated. An estimation of the lateral interactions was also achieved.

The values of $\Delta G^\circ_{ads}(H_{UPD})$, $\Delta H^\circ_{ads}(H_{UPD})$, and $\Delta S^\circ_{ads}(H_{UPD})$ were found to depend on the surface crystallographic orientation. The bond energy for H−Pt(*hkl*) electrodes obtained for Pt(111) and Pt(100) agree well with the UHV values.[32,35] Repulsive lateral interactions were found for both Pt(111) and Pt(100) from the dependence of the free energy change with coverage at constant temperature and were larger in the case of Pt(111), as expected on the basis of the shape of the voltammetric profiles.

By comparison with UHV data, it was concluded that the energetic effect of the double-layer rearrangement upon hydrogen adsorption, although existing, is not of great importance. However, the effect is significant on the adsorption entropy. The $\Delta S^\circ_{ads}(H_{UPD})$ values were found to be dependent on surface structure, − 48 J $mol^{-1}$ $K^{-1}$ for Pt(111), −56 J $mol^{-1}$ $K^{-1}$ for Pt(100), and from −55 to −70 J $mol^{-1}$ $K^{-1}$ for Pt(110) depending on coverage. These values (except for Pt(110) at some coverages) are intermediate between those of the limiting cases of immobile and mobile adlayers (in both cases, for an ideal one-component adsorption on an homogeneous surface). Assuming that the mobility of adsorbed H is severely restricted by the coadsorbed water, the difference between the experimental values and the theoretical ones for the immobile case have been attributed to changes in the double-layer structure (especially the water network in the inner layer) caused by H adsorption. This is justified, as these changes in the double layer are not included in the calculation of entropy for the immobile adlayer, which corresponds to a solid/gas interphase.

The disordering effect of hydrogen adsorption on the structure of the inner layer varies following the trend Pt(111) > Pt(100) > Pt(110). We believe that this is related to the initial degree of order in the water adlayer in the absence of adsorbed hydrogen. Geometrical arguments point to the fact that water adlayer acquires a more ordered structure on fcc(111) surfaces. Therefore, the possible disordering triggered by H adsorption should cause a larger effect on this surface.

Finally, we need to reconcile two pieces of information based on two different thermodynamic functions: small values for $\delta\Delta H^\circ_f(dl)$ and $(S^\circ_{dl'} - S^\circ_{dl}) > 0$. From the calculation of $\Delta H^\circ_{ads}(H_{UPD})$ and its comparison with values obtained from UHV experiments, it is concluded that the change in the double-layer structure caused by H adsorption does not imply an important change in the energetics of the inner layer. In other words, the adsorption of H does not alter significantly the average number of bonds per water (including hydrogen bonds to neighboring water molecules and Pt−water surface bonds). Seemingly, the adsorption of hydrogen weakens the Pt−$H_2O$ bond, but the energy lost in the weakening or rupture of the Pt−water bond would be replaced by a new hydrogen bond with neighboring water molecules in the solution side. Taking into account that both bonds have similar energies, the enthalpy of formation of the double-layer structure would not change in a significant way. On the other hand, the rupture (or weakening) of some Pt−water bonds upon H adsorption would increase the mobility of the water adlayer and therefore its entropy, leading to a positive value of $(S^\circ_{dl'} - S^\circ_{dl})$.

**Acknowledgment.** This work has been carried out in the framework of project BQU2000-0240 financed by the Ministerio de Ciencia y Tecnología (Spain) and projects GV01-401 and GV01-400 financed by Generalitat Valenciana. B.A. is grateful for the award of a Ph.D. grant from the Ministerio de Educación y Cultura (Spain).

## References and Notes

(1) (a) Clavilier, J. *J. Electroanal. Chem.* **1980**, *107*, 211. (b) Clavilier, J.; Faure, R.; Guinet, G.; Durand, R. *J. Electroanal. Chem.* **1980**, *107*, 205.

(2) *Interfacial Electrochemistry, Theory, Experiment and Applications*; Wieckowski, A., Ed.; Marcel Dekker: New York, 1999.

(3) MacDougall, B.; Conway, B. E.; Kozlowska, H. A. *J. Electroanal. Chem.* **1971**, *32*, App. 15.

(4) (a) Clavilier, J.; Albalat R.; Gómez, R.; Orts, J. M.; Feliu, J. M.; Aldaz, A. *J. Electroanal. Chem.* **1992**, *330*, 489. (b) Climent, V.; Gómez, R.; Orts, J. M.; Rodes, A.; Aldaz, A. In *Interfacial Electrochemistry, Theory, Experiment and Applications*; Wieckowski, A., Ed.; Marcel Dekker: New York, 1999; Chapter 26.

(5) Brown, G.; Rikvold, P. A.; Mitchell, S. J.; Novotny, M. A. In *Interfacial Electrochemistry, Theory, Experiment and Applications*; Wieckowski, A., Ed.; Marcel Dekker: New York, 1999; Chapter 4.

(6) Blum, L.; Legault, M. D.; Huckaby, D. A. In *Interfacial Electrochemistry, Theory, Experiment and Applications*; Wieckowski, A., Ed.; Marcel Dekker: New York, 1999; Chapter 2.

(7) (a) deBethune, A. J.; Licht, T. S.; Swendeman, N. *J. Electrochem. Soc.* **1959**, *106*, 616. (b) De Bethune, A. J.; Swendeman Loud, N. A. *Standard Aqueous Electrode Potentials and Temperature Coefficients at 25 °C*; Clifford A. Hampel: Skokie, IL, 1964.

(8) (a) Breiter, M. W. In *Transactions on the Symposium on Electrode Processes*; Yeager, E., Ed.; John Wiley & Sons: New York, 1961. (b) Breiter, M. *Electrochim. Acta* **1962**, *7*, 25. (c) Breiter, M. W. *Ann. N. Y. Acad. Sci.* **1963**, *101*, 709.

(9) Conway, B. E.; Angerstein-Kozlowska, H.; Sharp, W. B. A. *J. Chem. Soc., Faraday Trans. 1* **1978**, *74*, 1373.

(10) Ross, P. N. *Surf. Sci.* **1982**, *102*, 463.

(11) Ross, P. N. In *Chemistry and Physics of Solid Surfaces*; Vanselow. R., Howe, M., Eds.; Springer Series in Chemical Physics, Vol. 20; Springer-Verlag: Berlin, 1980; Vol. IV.

(12) Zolfaghari, A.; Jerkiewicz, G. *J. Electroanal. Chem.* **1997**, *420*, 11.

(13) Zolfaghari, A.; Jerkiewicz, G. *J. Electroanal. Chem.* **1997**, *422*, 1.

(14) Zolfaghari, A.; Jerkiewicz, G. *J. Electroanal. Chem.* **1999**, *467*, 177.

(15) Radovic-Hrapovic, Z.; Jerkiewicz, G. *J. Electroanal. Chem.* **2001**, *499*, 61.

(16) Markovic, N. M.; Schmidt, T. J.; Grgur, B. N.; Gasteiger, H. A.; Behm, R. J.; Ross, P. N. *J. Phys. Chem. B* **1999**, *103*, 8568.

(17) Zolfaghari, A.; Villiard, F.; Chayer, M.; Jerkiewicz, G. *J. Alloys Compd.* **1997**, *253−254*, 481.

(18) Clavilier, J.; Armand, D.; Sun, S. G.; Petit, M. *J. Electroanal. Chem.* **1986**, *205*, 266.
(19) Clavilier, J.; El Achi, K.; Petit, M.; Rodes, A.; Zamakhchari, A. *J. Electroanal. Chem.* **1990**, *295*, 333.
(20) Dickertmann, D.; Koppitz, F. D.; Schultze, J. W. *Electrochim. Acta* **1976**, *21*, 967.
(21) Pajkossy, T.; Kolb, D. M. *Electrochim. Acta* **2001**, *46*, 3063.
(22) Jerkiewicz, G.; Zolfaghari, A. *J. Phys. Chem.* **1996**, *100*, 8454.
(23) Love, B.; Seto, K.; Lipkowski, J. *Rev. Chem. Intermed.* **1987**, *8*, 87.
(24) (a) Conway, B. E.; Gileadi, E. *Trans. Faraday Soc.*, **1962**, *58*, 2493. (b) Conway, B. E.; Angerstein-Kozlowska, H.; Dhar, H. P. *Electrochim. Acta* **1974**, *19*, 455.
(25) Jerkiewicz, G. *Prog. Surf. Sci.* **1998**, *57*, 137.
(26) Pajkossy, T.; Kibler, L. A.; Kolb, D. M. *Electrochem. Commun.* **2002**, *4*, 787.
(27) Wagner, F. T. In *Structure of Electrified Interfaces*; Lipkowski, J., Ross, P. N., Eds.; VCH Publishers: New York, 1993.
(28) Wagner, F. T.; Moylan, T. E. *Surf. Sci.* **1987**, *182*, 125.
(29) Wagner, F. T.; Moylan, T. E. *Surf. Sci.* **1988**, *206*, 187.
(30) Chen, N.; Blowers, P.; Masel, R. I. *Surf. Sci.* **1999**, *419*, 150.
(31) *CRC Handbook of Chemistry and Physics*, 74th ed.; Lide, D. R., Ed.; CRC Press: Boca Raton, FL, 1993.
(32) Christmann, K. *Surf. Sci. Rep.* **1988**, *9*, 1.
(33) Podkolzin, S. G.; Watwe, R. M.; Yan, Q.; de Pablo, J. J.; Dumesic, J. A. *J. Phys. Chem. B* **2001**, *105*, 8550.
(34) Watson, G. W.; Welb, R. P. K.; Willock, D. J.; Hutchins, G. J. *J. Phys. Chem. B* **2001**, *105*, 4889.
(35) Christmann, K. In *Electrocatalysis*; Lipkowski, J., Ross, P. N., Eds.; Wiley-VCH: New York, 1998.
(36) Eisenberg, D.; Kauzmann, W. *The Structure and Properties of Water*; Oxford University Press: Oxford, U.K., 1969.
(37) (a) Adamson, A. W.; Gast, A. P. *Physical Chemistry of Surfaces*, 6th ed.; Wiley-Interscience: New York, 1997. (b) Hill, T. L. *An Introduction to Statistical Thermodynamics*; Dover Publications Inc.: New York, 1986.
(38) Nahm, T. V.; Gomer, R. *Surf. Sci.* **1997**, *375*, 281.
(39) Baró, A. M.; Ibach, H.; Bruchmann, H. D. *Surf. Sci.* **1979**, *88*, 384.
(40) Stenzel, W.; Jahnke, S. A.; Song, Y.; Conrad, H. *Prog. Surf. Sci.*, **1990**, *35*, 159.
(41) Breiter, M.; Kennel, B. *Z. Elektrochem.* **1960**, *64*, 1180.
(42) Clavilier, J.; Rodes, A.; El Achi, K.; Zamakhchari, M. *J. Chim. Phys.* **1991**, *88*, 1423.
(43) Zolfaghari, A.; Jerkiewicz, G. In *Electrochemical Surface Science of Hydrogen Adsorption and Absorption;* Jerkiewicz. G., Marcus, P., Eds.; The Electrochemistry Society: Pennington, NJ, 1997; PV 97−16.